Nonlinear Dyn (2020) 99:269–281
https://doi.org/10.1007/s11071-019-05198-w

ORIGINAL PAPER

Transient dynamics, damping, and mode coupling of nonlinear systems with internal resonances

Allen T. Mathis · D. Dane Quinn

Received: 18 December 2018 / Accepted: 16 August 2019 / Published online: 23 August 2019

Abstract The study of both linear and nonlinear structural vibrations routinely circles the concise yet complex problem of choosing a set of coordinates which yield simple equations of motion. In both experimental and mathematical methods, that choice is a difficult one because of measurement, computational, and interpretation difficulties. Often times, researchers choose to solve their problems in terms of linear, undamped mode shapes because they are easy to obtain; however, this is known to give rise to complicated phenomena such as mode coupling and internal resonance. This work considers the nature of mode coupling and internal resonance in systems containing non-proportional damping, linear detuning, and cubic nonlinearities through the method of multiple scales as well as instantaneous measures of effective damping. The energy decay observed in the structural modes is well approximated by the slow-flow equations in terms of the modal amplitudes, and it is shown how mode coupling enhances the dampingobserved in the system. Moreover, in the presence of a 3:1 internal resonance between two modes, the nonlinearities not only enhance the dissipation, but can allow for the exchange and transfer of energy between the resonant modes. However, this exchange depends on the resonant phase between the modes and is proportional to the energy in the lowest mode. The results of the analysis tie together interpretations used by both experimentalists and theoreticians to study such systems and provide a more concrete way to interpret these phenomena.

Keywords Nonlinear mode coupling · Transient dynamics · Equivalent damping · Multiple scales

This work is dedicated to the memory of Prof. Ali Hasan Nayfeh (1933–2017) in honor of his technical and personal contributions to the engineering dynamics community.

A. T. Mathis · D. D. Quinn (✉)
Department of Mechanical Engineering, The University of Akron, Akron, OH 44325–3903, USA
e-mail: quinn@uakron.edu

A. T. Mathis
e-mail: ata6@uakron.edu

1 Introduction

The central tenet of linear modal analysis is that the proper identification of mode shapes leads to the decoupling of modal equations of motion. For any generic, linear system,

$$\boldsymbol{M}\,\ddot{\mathbf{u}} + \boldsymbol{C}\,\dot{\mathbf{u}} + \boldsymbol{K}\,\mathbf{u} = \mathbf{0}, \tag{1}$$

the associated eigenproblem is given by

$$\left(\boldsymbol{K} + i\,\omega\,\boldsymbol{C} - \omega^2\,\boldsymbol{M}\right)\boldsymbol{\phi} = \mathbf{0}, \tag{2}$$

where $\mathbf{u}$ is the vector of physical coordinates, $\boldsymbol{M}$ is the mass matrix, $\boldsymbol{K}$ is the stiffness matrix, $\boldsymbol{C}$ is the damping matrix, $\boldsymbol{\phi}$ are the mode shapes, and ω are the natural frequencies. If the system is undamped, i.e., $\boldsymbol{C} = \mathbf{0}$, then solving Eq. (2) yields the real-valued, undamped mode

shapes and natural frequencies; however, if $\boldsymbol{C} \neq \boldsymbol{0}$, then the eigenproblem can yield complex mode shapes, appearing in complex conjugate pairs [4,5,10]. These calculations ultimately give real-valued displacements and decoupled equations of motion; however, often times in vibrations of continuous systems and/or experimental systems it is advantageous to use the undamped mode shapes, particularly because undamped mode shapes are easily measured from experimental data. Unfortunately one drawback of this approach is that applying a modal coordinate transformation based on the undamped mode shapes typically leads to coupling between the modes, i.e., the equations of motion are no longer decoupled in this case.

Additional difficulties in studying and understanding the nature of mode coupling and damping arise when one considers the wider class of nonlinear systems. With the inclusion of nonlinearities in the governing equations, in general a coordinate transformation no longer exists that can be used to decouple the equations of motion. However, the modal coordinates as identified from the corresponding linear system are nonetheless often used to simplify the equations of motion, so that in the resulting equations of motion coupling between the modal coordinates only occurs in the nonlinear terms [13]. The behavior of the system arising from this nonlinear coupling can exhibit energy dissipation rates that depend on the energy distribution within the system [8] as well as bifurcations not observed in the corresponding linear system [17,18]. Such behavior can play an important role in applications such as nanomechanical systems [9,11,12], thermoacoustic oscillations [14], and structural dynamics [15,22].

1.1 Equations of motion

We consider here a general nonlinear multi-degree-of-freedom system of the form

$$\boldsymbol{M}\,\ddot{\mathbf{u}} + \boldsymbol{C}\,\dot{\mathbf{u}} + \boldsymbol{K}\,\mathbf{u} + \mathbf{N}\,(\mathbf{u}, \dot{\mathbf{u}}) = \boldsymbol{0}, \tag{3}$$

where $\mathbf{N}$ is a vector containing the nonlinearities of the system. No set of linear mode shapes can be employed to decouple Eq. (3) for non-trivial, nonlinear $\mathbf{N}$; however, for weak nonlinearities perturbation methods can be employed to study the way those linear mode shapes are coupled together. The structure of the nonlinearities, $\mathbf{N}$, and their dependence on $\mathbf{u}$ and $\dot{\mathbf{u}}$ depend on the problem addressed, but in what follows $\mathbf{N}(\mathbf{u}, \dot{\mathbf{u}})$ is assumed to contain cubic stiffness and damping components while the linear damping is assumed small. As a result, the mass normalized mode shapes of the undamped linear system can be used to transform to modal coordinates, and the resulting equation of motion takes the form

$$\begin{aligned}\ddot{q}_i + \omega_i^2\, q_i + \epsilon \Bigg(& \sum_{j=1}^{N} \left[\lambda_{ij}\, \dot{q}_j + \xi_{ij}\, q_j\right] \\ & + \sum_{j=1}^{N}\sum_{k=1}^{N}\sum_{l=1}^{N} \Big[\mu^s_{ijkl}\, q_j q_k q_l + \mu^v_{ijkl}\, q_j q_k \dot{q}_l \\ & + \mu^d_{ijkl}\, \dot{q}_j\, \dot{q}_k\, \dot{q}_l + \mu^c_{ijkl}\, \dot{q}_j\, \dot{q}_k q_l\Big]\Bigg) = 0, \end{aligned} \tag{4}$$

with the modal coordinates $q_i(t)$ defined as

$$q_i(t) = \boldsymbol{\phi}_i^T\, \boldsymbol{M}\, \mathbf{u}(t). \tag{5}$$

In Eq. (4), $\epsilon \ll 1$ is a small parameter that characterizes the weakly nonlinear nature of the problem. The linear damping is described by the term $\lambda_{ij} \equiv \boldsymbol{\phi}_i^T\, \boldsymbol{C}\, \boldsymbol{\phi}_j$ while ξ_{ij} is included as a detuning in the linear stiffness from the $\epsilon = 0$ system based on the identified mode shapes. Both of these terms couple together the modal coordinates associated with the linear mode shape $\boldsymbol{\phi}_i$. In addition, modal coupling is introduced through the cubic nonlinearities. Here μ^s and μ^c describe nonlinear stiffness terms, with the former being a general cubic stiffness nonlinearity and the later representing a velocity-dependent term. Likewise, μ^v and μ^d are nonlinear damping terms. Many authors have studied these terms individually in the context of perturbation methods. In particular, the seminal work by Nayfeh and Mook [16] describes numerous examples of systems with small cubic stiffness nonlinearities, both with and without internal resonances. The cubic damping term described by μ^d is often associated with Rayleigh [1,3,19], while van der Pol type nonlinearities described by μ^v can arise in the study of mechanical, electrical, and biological systems [7]; both are dissipative in nature. The remaining nonlinearity of interest to this work, described by μ^c, can arise from geometric nonlinearities [6,20].

This work applies the method of multiple scales to develop approximate solutions to the modal equations that arise from multi-degree-of-freedom systems with general, non-proportional damping, detuning, and a broad class of cubic nonlinearities [16]. The real-valued, undamped mode shapes are used to decouple

the dominant, undamped, linear dynamics, as shown in Eq. (4). The dynamical response predicted by the averaged equations is shown to closely match numerical solutions of the original differential equations both when the modal frequencies are incommensurate and in the presence of internal resonances. While much of the related work in the literature has been concentrated in the study of one or two-degree-of-freedom systems, the results developed in this paper are scalable to arbitrary degrees of freedom. The resulting analysis describes the effect of the mistunings and nonlinearities on the amplitude of the linear modes and captures the effect of mode coupling on general multi-degree-of-freedom nonlinear systems.

1.2 Example system

While the focus of this work is the analysis of a general system of coupled equations including cubic nonlinearities, the results are applied to the finite-order modal expansion of a simply supported rectangular plate with point attachments undergoing infinitesimal deformation. The continuum plate is represented by

$$\begin{aligned}
&D\,\tilde{\nabla}^4\tilde{u} + (2\,\rho\,h)\,\tilde{u}_{\tilde{t}\tilde{t}} + \tilde{F}\,(\tilde{u}) = 0,\\
&\quad \tilde{x} \in [0, L_x], \quad \tilde{y} \in \left[0, L_y\right], \quad \tilde{t} > 0,\\
&\tilde{u}\left(0, \tilde{y}, \tilde{t}\right) = \tilde{u}\left(L_x, \tilde{y}, \tilde{t}\right) = \tilde{u}\left(\tilde{x}, 0, \tilde{t}\right)\\
&\quad = \tilde{u}\left(\tilde{x}, L_y, \tilde{t}\right) \equiv 0,\\
&\tilde{u}_{\tilde{x}\tilde{x}}\left(0, \tilde{y}, \tilde{t}\right) = \tilde{u}_{\tilde{x}\tilde{x}}\left(L_x, \tilde{y}, \tilde{t}\right) = \tilde{u}_{\tilde{x}\tilde{x}}\left(\tilde{x}, 0, \tilde{t}\right)\\
&\quad = \tilde{u}_{\tilde{x}\tilde{x}}\left(\tilde{x}, L_y, \tilde{t}\right) \equiv 0,\\
&\tilde{u}\,(\tilde{x}, \tilde{y}, 0) = \tilde{u}_0\,(\tilde{x}, \tilde{y})\,, \qquad \tilde{u}_{\tilde{t}}\,(\tilde{x}, \tilde{y}, 0) = \dot{\tilde{u}}_0(\tilde{x}, \tilde{y}),
\end{aligned} \tag{6}$$

where the tildes represent dimensional quantities, $\tilde{\nabla}^4$ is the biharmonic operator in dimensional coordinates, and $\tilde{F}$ is the term associated with the attachments, both linear and nonlinear. In this, ρ is the density and h is the plate thickness, while the flexural rigidity D is defined as

$$D = \frac{E\,h^3}{12\,(1-\nu^2)}, \tag{7}$$

with Young's modulus E and Poisson's ratio ν. Now consider the following nondimensionalization

$$x \equiv \frac{\pi\,\tilde{x}}{L_x}, \quad y \equiv \frac{\pi\,\tilde{y}}{L_x}, \quad u \equiv \frac{\tilde{u}}{U_\star}, \quad t = \frac{\tilde{t}}{\frac{L_x^2}{\pi^2}\sqrt{\frac{2\,\rho\,h}{D}}}, \tag{8}$$

where $U_\star$ is a characteristic displacement associated with the deformation. For example, if the initial energy in the system is identified as

$$\tilde{\mathcal{E}}(0) = \int_0^{L_y}\int_0^{L_x} \frac{1}{2}\left[(2\,\rho\,h)\,\left(\dot{\tilde{u}}_0\right)^2 + D\,\left(\tilde{\nabla}^2\tilde{u}_0\right)^2\right] \mathrm{d}x\,\mathrm{d}y, \tag{9}$$

then $U_\star$ can be chosen as

$$U_\star = \sqrt{\frac{\tilde{\mathcal{E}}(0)}{D\,L_x\,L_y}}. \tag{10}$$

Moreover, ϵ is a small parameter defined as

$$\epsilon \equiv \frac{F_\star\,L_x^4}{\pi^4\,D\,U_\star}, \tag{11}$$

where $F_\star$ is a nominal parameter associated with the strength of the attachments[1], and it is assumed that $\epsilon \ll 1$. Using this nondimensionalization, the problem reduces to

$$\begin{aligned}
&\nabla^4 u + u_{tt} + \epsilon F(u) = 0,\\
&\quad x \in [0, \pi], \quad y \in [0, \gamma\,\pi], \quad t > 0,\\
&u(0, y, t) = u(\pi, y, t) = u(x, 0, t)\\
&\quad = u(x, \gamma\,\pi, t) = 0,\\
&u_{xx}(0, y, t) = u_{xx}(\pi, y, t) = u_{xx}(x, 0, t)\\
&\quad = u_{xx}(x, \gamma\,\pi, t) = 0,\\
&u(x, y, 0) = u_0(x, y), \quad u_t(x, y, 0) = \dot{u}_0(x, y),
\end{aligned} \tag{12}$$

where $\gamma \equiv \frac{L_y}{L_x}$ is the aspect ratio of the plate, which can be varied to specify the modal frequencies and in particular examine resonant and non-resonant dynamics. For the nondimensionalized system, the mode shapes and natural frequencies to be used in the modal expansion are given by

$$\begin{aligned}
U_{m,n} &= 2\,\sin\,(m\,x)\,\sin\left(\frac{n\,y}{\gamma}\right),\\
\omega_{m,n} &= m^2 + \left(\frac{n}{\gamma}\right)^2.
\end{aligned} \tag{13}$$

The mistuning and nonlinearities are introduced through point attachments so that $F(u)$ takes the form

$$\begin{aligned}
F(u(x, y, t)) &= \lambda\,u_t(a_x, a_y, t)\,\delta(x - a_x)\,\delta(y - a_y)\\
&\quad + \xi\,u(b_x, b_y, t)\,\delta(x - b_x)\,\delta(y - b_y)
\end{aligned}$$

[1] One could, for example, choose $F_\star \equiv \tilde{F}(U_\star)$, so that $\epsilon \ll 1$ implies that $\tilde{F}(U_\star) \ll (\pi/L_x)^4\,D\,U_\star$, although other choices can also be used to nondimensionalize the system.

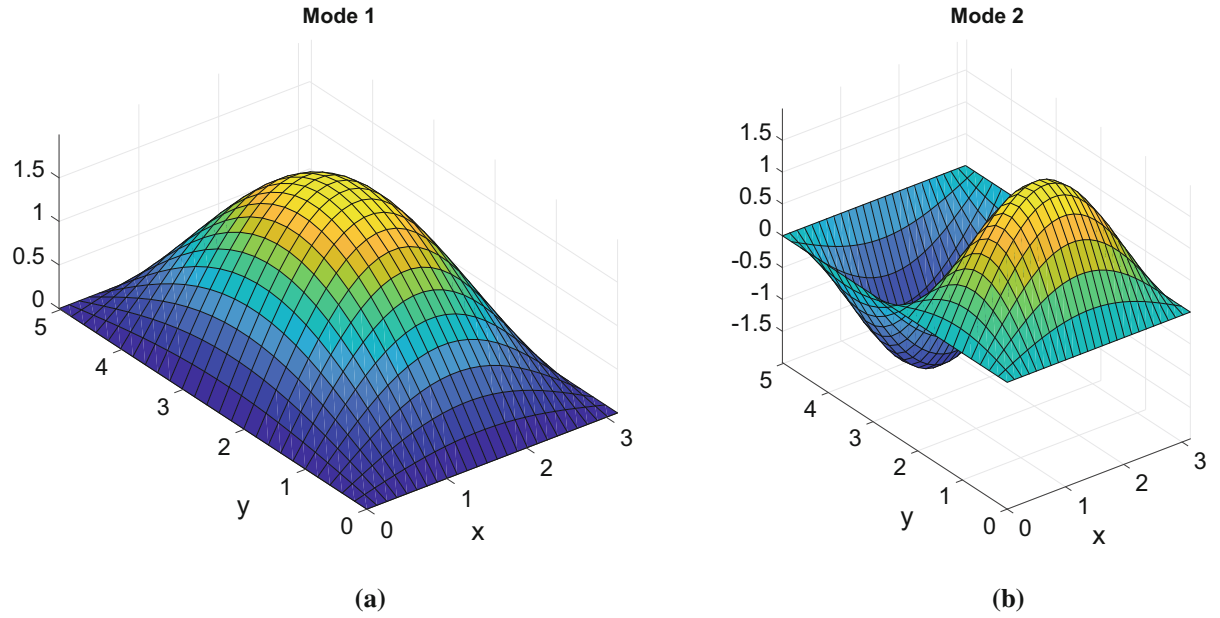

Fig. 1 Linear mode shapes, non-commensurate frequencies ($\gamma = 1.6$); **a** Mode 1—$m = 1, n = 1$, **b** Mode 2—$m = 1, n = 2$

$$
\begin{aligned}
&+\mu^s\, u^3(c_x, c_y, t)\, \delta(x - c_x)\, \delta(y - c_y)\\
&+\mu^v\, u^2(d_x, d_y, t)\, u_t(d_x, d_y, t)\, \delta(x - e_x)\, \delta(y - e_y)\\
&+\mu^c\, u(f_x, f_y, t)\, u_t^2(f_x, f_y, t)\, \delta(x - f_x)\, \delta(y - f_y)\\
&+\mu^d\, u_t^3(d_x, d_y, t)\, \delta(x - d_x)\, \delta(y - d_y). \qquad (14)
\end{aligned}
$$

Physically $F(u)$ describes a linear damper located at (a_x, a_y), a linear spring at (b_x, b_y), and cubic nonlinearities located at corresponding points on the rectangular plate. Using the specified undamped linear modes as basis functions for a Galerkin method, the modal equations for this rectangular plate reduce to Eq. (4) where the constant coefficients are calculated to be

$$
\begin{aligned}
\lambda_{ij} &= \lambda \cdot U_i(a_x, a_y)\, U_j(a_x, a_y),\\
\xi_{ij} &= \xi\, U_i(b_x, b_y)\, U_j(b_x, b_y),\\
\mu^s_{ijkl} &= \mu^s \cdot U_i(c_x, c_y)\, U_j(c_x, c_y) U_k(c_x, c_y) U_l(c_x, c_y),\\
\mu^v_{ijkl} &= \mu^v \cdot U_i(e_x, e_y)\, U_j(e_x, e_y) U_k(e_x, e_y) U_l(e_x, e_y),\\
\mu^c_{ijkl} &= \mu^c \cdot U_i(f_x, f_y)\, U_j(f_x, f_y) U_k(f_x, f_y) U_l(f_x, f_y),\\
\mu^d_{ijkl} &= \mu^d \cdot U_i(d_x, d_y)\, U_j(d_x, d_y) U_k(d_x, d_y) U_l(d_x, d_y). \qquad (15)
\end{aligned}
$$

Note that for a specific set of indices (i, j, k, l) all permutations of these coefficients are identical, e.g., $\mu^s_{ijkl} = \mu^s_{lkji} = \mu^s_{jlki} = \cdots$.

In the examples that follow, a two mode expansion for Eq. (12) will be considered, keeping modes $(m, n) = (1, 1)$ and $(m, n) = (1, 2)$ as shown in Fig. 1. In addition, the attachments described in Eq. (14) are assumed to be collocated at $(x, y) = (\pi/2, 3\,\gamma\,\pi/8)$, so that they are neither at a node nor maximum point of either mode. The value of γ will be chosen to set the resonance relation between the modes of interest. The small parameter is chosen to be $\epsilon = 0.10$ and unless noted the attachment parameters are assumed to be

$$
\begin{aligned}
&\lambda = 0.25, \quad \xi = 0.00, \quad \mu^s = 0.25,\\
&\mu^d = 0.25, \quad \mu^v = 0.25, \quad \mu^c = 0.25. \qquad (16)
\end{aligned}
$$

The resulting parameters in the modal equations are determined from Eq. (15).

2 Asymptotic solution

The method of multiple scales is applied to develop an asymptotic solution. Specifically, the modal coordinates $q_i(t)$ are expanded in the small parameter ϵ as

$$
q_i(t) = q_i^{(0)}(t) + \epsilon\, q_i^{(1)}(t) + \epsilon^2\, q_i^{(2)}(t) + \cdots, \qquad (17)
$$

together with the identification of the time scales $\eta_i \equiv \epsilon^i\, t$, such that

$$
\eta_0 = t, \quad \eta_1 = \epsilon\, t, \quad \eta_2 = \epsilon^2\, t. \qquad (18)
$$

As a result, time derivatives are expanded as

$$\frac{d}{dt} = \frac{\partial}{\partial \eta_0} + \epsilon \frac{\partial}{\partial \eta_1} + \epsilon^2 \frac{\partial}{\partial \eta_2} + \cdots, \tag{19a}$$

$$\frac{d^2}{dt^2} = \frac{\partial^2}{\partial \eta_0^2} + \epsilon \left[2 \frac{\partial^2}{\partial \eta_0 \, \partial \eta_1} \right] + \epsilon^2 \left[\frac{\partial^2}{\partial \eta_1^2} + 2 \frac{\partial^2}{\partial \eta_0 \, \partial \eta_2} \right] + \cdots. \tag{19b}$$

Introducing these into Eq. (4), the $\mathcal{O}(1)$ terms in the expansion reduce to

$$\frac{\partial^2 q_i^{(0)}}{\partial \eta_0^2} + \omega_i^2 \, q_i^{(0)} = 0, \tag{20}$$

for each mode, leading to the general solution

$$q_i^{(0)} = A_i^{(0)} \left(\boldsymbol{\eta}_1 \right) \, \sin \left(\omega_i \, \eta_0 + \phi_i^{(0)} \left(\boldsymbol{\eta}_1 \right) \right). \tag{21}$$

Here the notation $\boldsymbol{\eta}_1$ indicates dependence on all times scales at or slower than η_1, that is $\boldsymbol{\eta}_1 \equiv (\eta_1, \eta_2, \ldots)$. Note that in particular at this order of the asymptotic approximation the individual modes remain uncoupled on the η_0 time scale. Mode coupling will arise in the slow time dynamics of the amplitude and phase terms, that is, $A_i^{(0)} \left(\boldsymbol{\eta}_1 \right)$ and $\phi_i^{(0)} \left(\boldsymbol{\eta}_1 \right)$, respectively.

The $\mathcal{O}(\epsilon)$ terms can then be written as

$$\begin{aligned} &\frac{\partial^2 q_i^{(1)}}{\partial \eta_0^2} + \omega_i^2 \, q_i^{(1)} + 2 \frac{\partial^2 q_i^{(0)}}{\partial \eta_0 \, \partial \eta_1} \\ &+ \sum_{j=1}^{N} \left[\lambda_{ij} \frac{\partial q_j^{(0)}}{\partial \eta_0} + \xi_{ij} \, q_j^{(0)} \right] \\ &+ \sum_{j=1}^{N} \sum_{k=1}^{N} \sum_{l=1}^{N} \Big[\mu_{ijkl}^{s} \, q_j^{(0)} \, q_k^{(0)} q_l^{(0)} \\ &+ \mu_{ijkl}^{c} \frac{\partial q_j^{(0)}}{\partial \eta_0} \frac{\partial q_k^{(0)}}{\partial \eta_0} \, q_l^{(0)} \\ &+ \mu_{ijkl}^{v} \, q_j^{(0)} \, q_k^{(0)} \frac{\partial q_l^{(0)}}{\partial \eta_0} \\ &+ \mu_{ijkl}^{d} \frac{\partial q_j^{(0)}}{\partial \eta_0} \frac{\partial q_k^{(0)}}{\partial \eta_0} \frac{\partial q_l^{(0)}}{\partial \eta_0} \Big] = 0. \end{aligned} \tag{22}$$

The multiple scale analysis proceeds by removing secular terms from the above equation, so that the coefficients of harmonic terms with frequency ω_i vanish. The resulting slow-flow equations can be written as

$$\cos \left(\omega_i \, \eta_0 + \phi_i^{(0)} \right): \qquad 2 \, \omega_i \, \frac{\partial A_i^{(0)}}{\partial \eta_1} + \lambda_{ii} \, \omega_i \, A_i^{(0)} + a_{i1} = 0, \tag{23a}$$

$$\sin \left(\omega_i \, \eta_0 + \phi_i^{(0)} \right): \quad -2 \, \omega_i \, A_i^{(0)} \, \frac{\partial \phi_i^{(0)}}{\partial \eta_1} + \xi_{ii} \, A_i^{(0)} + b_{i1} = 0, \tag{23b}$$

where a_{i1} and b_{i1} represent the cosine and sine components of the cubic nonlinearities averaged over one period of mode i and are given by

$$\begin{aligned} a_{i1} = \sum_{j=1}^{N} \sum_{k=1}^{N} \sum_{l=1}^{N} \Big\{ A_j^{(0)} \, A_k^{(0)} \, A_l^{(0)} \Big[&\mu_{ijkl}^{s} \, I_{ijkl}^{s,\cos} \\ &+ \omega_l \, \mu_{ijkl}^{v} \, I_{ijkl}^{v,\cos} \\ &+ \omega_j \, \omega_k \, \omega_l \, \mu_{ijkl}^{d} \, I_{ijkl}^{d,\cos} + \omega_j \, \omega_k \, \mu_{ijkl}^{c} \, I_{ijkl}^{c,\cos} \Big] \Big\}, \end{aligned} \tag{24a}$$

$$\begin{aligned} b_{i1} = \sum_{j=1}^{N} \sum_{k=1}^{N} \sum_{l=1}^{N} \Big\{ A_j^{(0)} \, A_k^{(0)} \, A_l^{(0)} \Big[&\mu_{ijkl}^{s} \, I_{ijkl}^{s,\sin} \\ &+ \omega_l \, \mu_{ijkl}^{v} \, I_{ijkl}^{v,\sin} \\ &+ \omega_j \, \omega_k \, \omega_l \, \mu_{ijkl}^{d} \, I_{ijkl}^{d,\sin} + \omega_j \, \omega_k \, \mu_{ijkl}^{c} \, I_{ijkl}^{c,\sin} \Big] \Big\}. \end{aligned} \tag{24b}$$

The coefficients $I_{ijkl}^{\bullet,\bullet}$, defined in "Appendix A", describe the contributions of resonant terms that depend on the modal frequencies of the system. These terms typically vanish unless specific resonance conditions hold, as illustrated below.

The mechanical energy present in a mode is related to the amplitude as

$$\mathcal{E}_i = \frac{\left(\omega_i \, A_i^{(0)} \right)^2}{2}, \tag{25}$$

so that to lowest order the time derivative of the modal energy is

$$\frac{d\mathcal{E}_i}{dt} = \epsilon \, \omega_i^2 \, A_i^{(0)} \, \frac{\partial A_i^{(0)}}{\partial \eta_1} = - \epsilon \left[\lambda_{ii} \, \mathcal{E}_i + \frac{\omega_i \, A_i^{(0)}}{2} \, a_{i1} \right]. \tag{26}$$

2.1 Non-commensurate modes

In the absence of an internal resonance between the linear modes, the frequencies of the system are non-commensurate, that is $\omega_i \neq \omega_j$ for all $i \neq j$. Therefore, the coefficients $I_{ijkl}^{\bullet,\bullet}$ given in Appendix A can be

evaluated so that the slow-flow equations can be written as

$$\frac{\partial A_i^{(0)}}{\partial \eta_1} + \left(\frac{\lambda_{ii}}{2}\right) A_i^{(0)} + \left\{\left(\frac{\mu^v_{iiii}}{8}\right)\left(A_i^{(0)}\right)^3 + \sum_{j\neq i}\left(\frac{\mu^v_{ijji}}{4}\right) A_i^{(0)}\left(A_j^{(0)}\right)^2\right\} + \left\{\left(\frac{3\,\mu^d_{iiii}\,\omega_i^2}{8}\right)\left(A_i^{(0)}\right)^3 + \sum_{j\neq i}\left[\left(\frac{\left(\mu^d_{iijj}+\mu^d_{ijij}+\mu^d_{ijji}\right)\omega_j^2}{4}\right) A_i^{(0)}\left(A_j^{(0)}\right)^2\right]\right\} = 0, \tag{27a}$$

$$\frac{\partial \phi_i^{(0)}}{\partial \eta_1} - \frac{\xi_{ii}}{2\,\omega_i} - \left\{\left(\frac{\mu^c_{iiii}\omega_i}{8}\right)\left(A_i^{(0)}\right)^2 + \sum_{j\neq i}\left(\frac{\mu^c_{ijji}\,\omega_j^2}{4\omega_i}\right)\left(A_j^{(0)}\right)^2 + \left(\frac{3\,\mu^s_{iiii}}{8\,\omega_i}\right)\left(A_i^{(0)}\right)^2 + \sum_{j\neq i}\left[\left(\frac{\left(\mu^s_{iijj}+\mu^s_{ijij}+\mu^s_{ijji}\right)}{4\,\omega_i}\right)\left(A_j^{(0)}\right)^2\right]\right\} = 0. \tag{27b}$$

In particular, the amplitude equations can be reformulated as

$$\begin{bmatrix} \frac{\partial A_1^{(0)}}{\partial \eta_1} \\ \vdots \\ \frac{\partial A_i^{(0)}}{\partial \eta_1} \\ \vdots \\ \frac{\partial A_N^{(0)}}{\partial \eta_1} \end{bmatrix} + \frac{1}{2}\begin{bmatrix} \Lambda_{11} & 0 & \dots & \dots & 0 \\ 0 & \ddots & \ddots & & \vdots \\ \vdots & \ddots & \Lambda_{ii} & \ddots & \vdots \\ \vdots & & \ddots & \ddots & 0 \\ 0 & \dots & \dots & 0 & \Lambda_{NN} \end{bmatrix}\begin{bmatrix} A_1^{(0)} \\ \vdots \\ A_i^{(0)} \\ \vdots \\ A_N^{(0)} \end{bmatrix} = \begin{bmatrix} 0 \\ \vdots \\ 0 \\ \vdots \\ 0 \end{bmatrix}, \tag{28}$$

where

$$\Lambda_{ii} \equiv \lambda_{ii} + \left[\frac{\mu^v_{iiii} + 3\,\mu^d_{iiii}\,\omega_i^2}{2\,\omega_i^2}\right]\mathcal{E}_i + \sum_{j\neq i}\left\{\left[\frac{\mu^v_{iijj} + 3\,\mu^d_{iijj}\,\omega_j^2}{\omega_j^2}\right]\mathcal{E}_j\right\}, \tag{29}$$

and for the nonlinear coefficients given in Eq. (15), $\mu^d_{iijj} = \mu^d_{ijij} = \mu^d_{ijji}$. With Γ_i identified as the instantaneous damping of the i-th mode of the system, for non-commensurate modes $\Gamma_i \equiv \Lambda_{ii}$, the nonlinear extension of the damping coefficient in a linear system.

The energy in the i-th mode is governed by the equation

$$\frac{\mathrm{d}\mathcal{E}_i}{\mathrm{d}t} = -\epsilon\,\Lambda_{ii}\,\mathcal{E}_i, \tag{30}$$

where Λ_{ii} depends on the energy in each mode. Note that for linear damping only the coefficients along the diagonal of the linear damping matrix contribute to the lowest-order decay of the amplitude. The off-diagonal terms that describe non-proportional damping and represent mode coupling through the damping are absent to $\mathcal{O}(\epsilon)$. Thus the response of a linear system with non-proportional damping is approximated to lowest order with simply modal damping, obtained by ignoring the off-diagonal components. This result has been observed in other contexts as well. For example, Bilbao et al. [2] show in their work how the non-proportional damping matrix of a finite element model can be approximated by a proportional one by minimizing the difference in energy dissipation between the two systems, while Udwadia [21] discusses minimizing the Euclidean norm of the difference between a non-proportional modal damping matrix and its approximation. The net result of these approximations for any non-proportional damping is simply to ignore the off-diagonal entries of $\boldsymbol{\Lambda}$ and retain only the elements along the diagonal leading to a form identical to that developed above. These approaches are computationally efficient and describe the lowest-order contribution from linear damping.

With the introduction of nonlinearities, this measure of the instantaneous damping given by Λ_{ii} is no longer constant, but rather depends on the squared amplitude of the modes of the system, corresponding to the distribution of the energy through the modes of the system. Hence the response of each mode is coupled to the remainder. However, because of the symmetric nature of the μ_{ijkl} terms, for the case of non-commensurate natural frequencies, $\Lambda_{ii} > 0$ provided that $\mu^{(c,s)}_{ijkl} > 0$, which corresponds to positive damping. Therefore, although the modes are coupled together through damping, the energy in any given mode cannot increase due to this mode

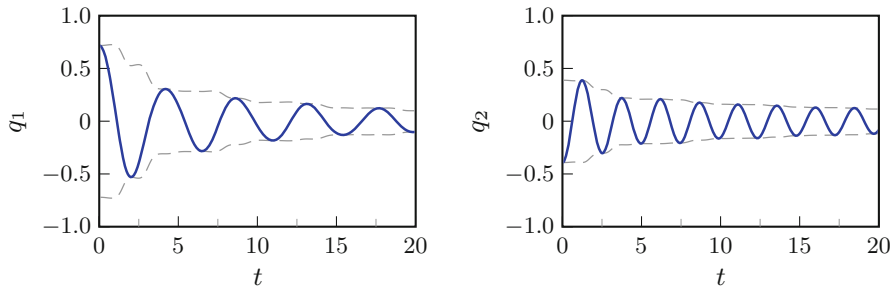

Fig. 2 Modal response ($\gamma = 1.60$); $(\mathcal{E}_1(0), \mathcal{E}_2(0)) = (0.50, 0.50)$. The dashed line represents the amplitude as derived from the energy, that is, $A_i^{(0)}$ from Eq. (25)

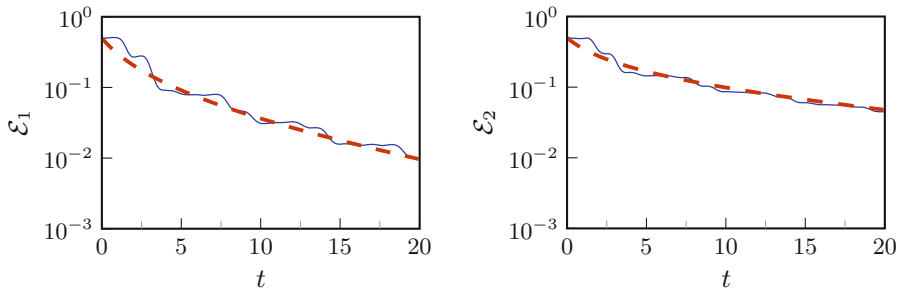

Fig. 3 Modal energies ($\gamma = 1.60$, $(\mathcal{E}_1(0), \mathcal{E}_2(0)) = (0.50, 0.50)$); Original Equations: blue solid line, Averaged Equations: red solid spaced line (Color figure online)

coupling, that is, the energy cannot be transferred from one mode to another in the absence of an internal resonance. Instead, the effect of mode coupling is to increase the overall dissipation observed in this system, as compared to the corresponding nonlinear system in which the mode coupling is neglected.

The phase variables are likewise reformulated as

$$\begin{bmatrix} \frac{\partial \phi_1^{(0)}}{\partial \eta_1} \\ \vdots \\ \frac{\partial \phi_i^{(0)}}{\partial \eta_1} \\ \vdots \\ \frac{\partial \phi_N^{(0)}}{\partial \eta_1} \end{bmatrix} = \begin{bmatrix} \Omega_{11} & 0 & \dots & \dots & 0 \\ 0 & \ddots & \ddots & & \vdots \\ \vdots & \ddots & \Omega_{ii} & \ddots & \vdots \\ \vdots & & \ddots & \ddots & 0 \\ 0 & \dots & \dots & 0 & \Omega_{NN} \end{bmatrix} \tag{31}$$

with

$$\Omega_{ii} \equiv \frac{\xi_{ii}}{2\,\omega_i} + \left[\frac{\mu^c_{iiii}\,\omega_i^2 + 3\,\mu^s_{iiii}}{4\,\omega_i^3}\right]\mathcal{E}_i + \sum_{j\neq i}\left\{\left[\frac{\mu^c_{ijji}\,\omega_j^2 + 3\,\mu^s_{iijj}}{2\,\omega_i\,\omega_j^2}\right]\mathcal{E}_j\right\}, \tag{32}$$

where $\mu^s_{iijj} = \mu^s_{ijij} = \mu^s_{ijji}$. The $\mathcal{O}(\epsilon)$ frequency shift of the i-the mode is described by Ω_{ii}, and as with the decay rate, the shift due to the nonlinearities depends on the energy in each mode. Finally, the decay in the amplitude of the response is independent of the phase of the corresponding mode. Once the energy in each mode is determined from Eqs. (27)a and (25), the phase variables can be solved from Eq. (27)b by quadrature.

Consider the two mode expansion of the plate described above with $\gamma = 1.60$. This aspect ratio was chosen so that the frequencies are not commensurate and reduce to

$$\omega_1 \equiv \omega_{1,1} = 1 + \frac{1}{\gamma^2} \approx 1.3906,$$
$$\omega_2 \equiv \omega_{1,2} = 1 + \frac{4}{\gamma^2} \approx 2.5625. \tag{33}$$

The initial conditions are chosen so that the initial energy in each mode is identical, with $\mathcal{E}_1(0) = \mathcal{E}_2(0) = 0.50$. For the direct numerical simulation of the original equations of motion, the initial conditions are chosen to be

$$q_1(0) = q_2(0) = 0, \quad \dot{q}_1(0) = \dot{q}_2(0) = \frac{\sqrt{2}}{2}, \tag{34}$$

while those of the averaged equations given in Eq. (28) are

$$A_1^{(0)}(0) = \frac{\sqrt{2}}{2\,\omega_1}, \quad A_2^{(0)}(0) = \frac{\sqrt{2}}{2\,\omega_2}. \tag{35}$$

The modal response for this system is shown in Fig. 2 when the initial energy is equally distributed between the two modes. For reference in each figure, the amplitude as derived from the energy in the appropriate mode

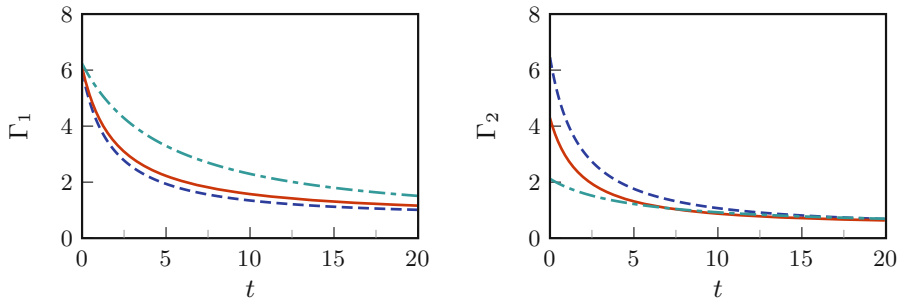

Fig. 4 Instantaneous damping, varying energy ratio ($\gamma = 1.60$); $(\mathcal{E}_1(0), \mathcal{E}_2(0)) = (0.99, 0.01)$: blue dashed line, $(\mathcal{E}_1(0), \mathcal{E}_2(0)) = (0.50, 0.50)$: red solid line, $(\mathcal{E}_1(0), \mathcal{E}_2(0)) = (0.01, 0.99)$: green solid dotted line (Color figure online)

as given in Eq. (25) is shown with the dashed line. Likewise, the evolution of the energy in each mode is shown in Fig. 3 for both the numerical simulation of the original equations of motion and the approximation from the averaged equations. The agreement between the two is excellent, and in particular the averaged response captures the slowly varying decay of the energy in each mode. In addition, as shown in Fig. 4 the instantaneous damping as defined by Γ_i from Eq. (29) can be predicted by the multiple scales analysis. As the energy distribution is varied, the nonlinear damping is seen to play a significant role in the observed response of the system. As a reminder, with linear damping alone the instantaneous damping would be constant and equal to the diagonal damping element λ_{ii}. However, as predicted by the multiple scales analysis the instantaneous damping depends significantly on the energy in the response. Moreover, even in the absence of an internal resonance the energy decay in each mode depends not only on the energy in that mode, but in the energy distribution throughout the system due to the mode coupling evidenced by the summation in Eq. (29). Notably, in this example the higher mode corresponding to Γ_2 is most sensitive to the energy distribution in the system.

2.2 3:1 Internal resonance

In the presence of nonlinearities, resonant conditions between the frequencies of the linear modes can give rise to additional secular terms in Eq. (22). In particular, if there exists a 3:1 resonance, between modes α and β, so that $3\,\omega_\alpha - \omega_\beta = \mathcal{O}(\epsilon)$, the cubic nonlinearities couple together the resonant modes, so that the slow-flow equations can be written as

$$\begin{bmatrix} \frac{\partial A_1^{(0)}}{\partial \eta_1} \\ \vdots \\ \frac{\partial A_\alpha^{(0)}}{\partial \eta_1} \\ \frac{\partial A_\beta^{(0)}}{\partial \eta_1} \\ \vdots \\ \frac{\partial A_i^{(0)}}{\partial \eta_1} \end{bmatrix} + \frac{1}{2} \begin{bmatrix} \Lambda_{11} & 0 & \dots & \dots & \dots & 0 \\ 0 & \ddots & \ddots & & & \vdots \\ \vdots & 0 & \Lambda_{\alpha\alpha} & \Lambda_{\alpha\beta} & 0 & \vdots \\ \vdots & 0 & \Lambda_{\beta\alpha} & \Lambda_{\beta\beta} & 0 & \vdots \\ \vdots & & & & \ddots & 0 \\ 0 & \dots & \dots & \dots & 0 & \Lambda_{NN} \end{bmatrix} \begin{bmatrix} A_1^{(0)} \\ \vdots \\ A_\alpha^{(0)} \\ A_\beta^{(0)} \\ \vdots \\ A_N^{(0)} \end{bmatrix} = \begin{bmatrix} 0 \\ \vdots \\ 0 \\ 0 \\ \vdots \\ 0 \end{bmatrix} \tag{36}$$

where Λ_{ii} is given in Eq. (29) and

$$\Lambda_{\alpha\beta} \equiv \frac{\mathcal{E}_\alpha}{2\,\omega_\alpha^3} \left\{ \left[3\,\mu^s_{\alpha\alpha\alpha\beta} + 5\,\omega_\alpha^2\,\mu^c_{\alpha\alpha\alpha\beta} \right] \sin\left(\psi^{(0)}_{\alpha\beta}\right) + \left[-\omega_\alpha\,\mu^v_{\alpha\alpha\alpha\beta} + 9\,\omega_\alpha^3\,\mu^d_{\alpha\alpha\alpha\beta} \right] \cos\left(\psi^{(0)}_{\alpha\beta}\right) \right\}, \tag{37a}$$

$$\Lambda_{\beta\alpha} \equiv \frac{\mathcal{E}_\alpha}{6\,\omega_\alpha^3} \left\{ \left[-\mu^s_{\alpha\alpha\alpha\beta} + \omega_\alpha^2\,\mu^c_{\alpha\alpha\alpha\beta} \right] \sin\left(\psi^{(0)}_{\alpha\beta}\right) + \left[-\omega_\alpha\,\mu^v_{\alpha\alpha\alpha\beta} + \omega_\alpha^3\,\mu^d_{\alpha\alpha\alpha\beta} \right] \cos\left(\psi^{(0)}_{\alpha\beta}\right) \right\}, \tag{37b}$$

with $\psi^{(0)}_{\alpha\beta} \equiv 3\,\phi^{(0)}_\alpha - \phi^{(0)}_\beta$. In the presence of the internal resonance between modes α and β, note that only the evolution equations for modes α and β are altered; the remaining non-resonant modes ($i \neq (\alpha, \beta)$) remain unchanged from those observed in Eq. (28). These off-diagonal coupling terms are non-reciprocal, so that $\Lambda_{\alpha\beta} \neq \Lambda_{\beta\alpha}$, while these equivalent damping coefficients depend only on $\mathcal{E}_\alpha$, the energy in the resonant

mode with the lowest frequency. Thus, if the lowest frequency mode is unexcited, the system cannot transfer energy from the higher mode, but the converse does not hold. If the system is excited in the lower mode, energy can be transferred to the higher resonant mode.

In contrast to the previously considered case with non-commensurate frequencies, the resonant phase $\psi^{(0)}_{\alpha\beta}$ influences the coupling between the resonant amplitudes, and therefore the energy distribution in these modes. Moreover, these coupling terms can be of either sign depending on this phase. Thus the presence of the 3 : 1 internal resonance makes possible the exchange of energy between the resonant modes. This is in contrast to the non-resonant modes, where Λ_{ii} is always positive for positive damping coefficients, so that the presence of the nonlinearities can enhance the dissipation but cannot lead to an energy increase in a mode due to energy exchange.

The phase equations for the non-resonant modes are identical to those given in Eq. (27b), while for the resonant modes α and β are expressed as

$$\frac{\partial \phi^{(0)}_{\alpha}}{\partial \eta_1} = \Omega_{\alpha\alpha} - \Omega_{\alpha\beta}, \tag{38a}$$

$$\frac{\partial \phi^{(0)}_{\beta}}{\partial \eta_1} = -\Omega_{\beta\alpha} + \Omega_{\beta\beta}, \tag{38b}$$

with

$$\Omega_{\alpha\beta} = \left\{\left[3\,\mu^{s}_{\alpha\alpha\alpha\beta} - 5\,\omega^2_{\alpha}\,\mu^{c}_{\alpha\alpha\alpha\beta}\right]\cos\left(\psi^{(0)}_{\alpha\beta}\right) + \left[-\omega_{\alpha}\,\mu^{v}_{\alpha\alpha\alpha\beta} + 3\,\omega^2_{\alpha}\,\mu^{d}_{\alpha\alpha\alpha\beta}\right]\sin\left(\psi^{(0)}_{\alpha\beta}\right)\right\}\frac{A^{(0)}_{\alpha}\,A^{(0)}_{\beta}}{8\,\omega_{\alpha}}, \tag{39a}$$

$$\Omega_{\beta\alpha} = \left\{\left[-\mu^{s}_{\alpha\alpha\alpha\beta} + \omega^2_{\alpha}\,\mu^{c}_{\alpha\alpha\alpha\beta}\right]\cos\left(\psi^{(0)}_{\alpha\beta}\right) + \left[\omega_{\alpha}\,\mu^{v}_{\alpha\alpha\alpha\beta} - \omega^3_{\alpha}\,\mu^{d}_{\alpha\alpha\alpha\beta}\right]\sin\left(\psi^{(0)}_{\alpha\beta}\right)\right\}\frac{\left(A^{(0)}_{\alpha}\right)^3}{24\,\omega_{\alpha}\,A^{(0)}_{\beta}}, \tag{39b}$$

and the evolution of the resonant phase $\psi^{(0)}_{\alpha\beta}$ is governed by

$$\frac{\partial \psi^{(0)}_{\alpha\beta}}{\partial \eta_1} = 3\,\frac{\partial \phi^{(0)}_{\alpha}}{\partial \eta_1} - \frac{\partial \phi^{(0)}_{\beta}}{\partial \eta_1}. \tag{40}$$

As with the amplitudes, the coupling in the phase evolution is non-reciprocal.

The effective damping of a mode is typically defined in terms of the instantaneous decay rate of the corresponding amplitude. In particular, such a definition cannot distinguish between damping, which is intrinsic to the mode and always negative, from energy transfer, which represents the flow of energy between modes and can be positive or negative depending on the coupling. In this context the amplitude equations for the resonant modes can be written as

$$\frac{\partial A^{(0)}_{\alpha}}{\partial \eta_1} + \underbrace{\frac{1}{2}\left(\Lambda_{\alpha\alpha} + \Lambda_{\alpha\beta}\,\frac{A^{(0)}_{\beta}}{A^{(0)}_{\alpha}}\right)}_{\text{Effective Damping, } \Gamma_{\alpha}} A^{(0)}_{\alpha},$$

$$\frac{\partial A^{(0)}_{\beta}}{\partial \eta_1} + \underbrace{\frac{1}{2}\left(\Lambda_{\beta\alpha}\,\frac{A^{(0)}_{\alpha}}{A^{(0)}_{\beta}} + \Lambda_{\beta\beta}\right)}_{\text{Effective Damping, } \Gamma_{\beta}} A^{(0)}_{\beta}. \tag{41}$$

where the effective damping for modes α and β reflects the coupling between these modes. Note that these effective damping measures depend on the energy in each mode and for mode β can be singular when $A^{(0)}_{\beta} = 0$ although the lower mode α is always finite because of the dependence of $\Lambda_{\alpha\beta}$ on the energy of this mode. The effective damping for the non-commensurate frequencies remains unchanged.

In the following examples, the plate described above is used with $\gamma = \frac{\sqrt{2}}{2}$, so that the natural frequencies of the two modes considered exhibit a 3 : 1 resonance, with $\omega_1 = 3$ and $\omega_2 = 9$. The response of the system will be considered as both the initial energy distribution between the resonant modes varies and the initial resonant phase of the system. The examples consider intermediate total energy levels, so that the nonlinearity is expected to influence the response of the system, while the total energy in the resonant modes is held constant, so that $\mathcal{E}_1(0) + \mathcal{E}_2(0) = 1.00$.

As shown in Fig. 5, the decay of the modal energies from the direct numerical simulation of the original equations of motion, shown in blue, is well approximated by the prediction from the multiple scales analysis (dashed red). The decay rate as identified in Eq. (41) depends on the energy distribution in the system, as shown in Fig. 6. However, unlike the previous results in which Γ_i was always positive for positive damping, the additional mode coupling introduced by Λ_{12} and Λ_{21} can lead to energy transfer between modes. This is best illustrated with $(\mathcal{E}_1(0), \mathcal{E}_2(0)) = (0.99, 0.01)$ with the response shown in Fig. 5c. As seen in Fig. 6b, Γ_2 for this initial state, the energy in Mode 2 initially

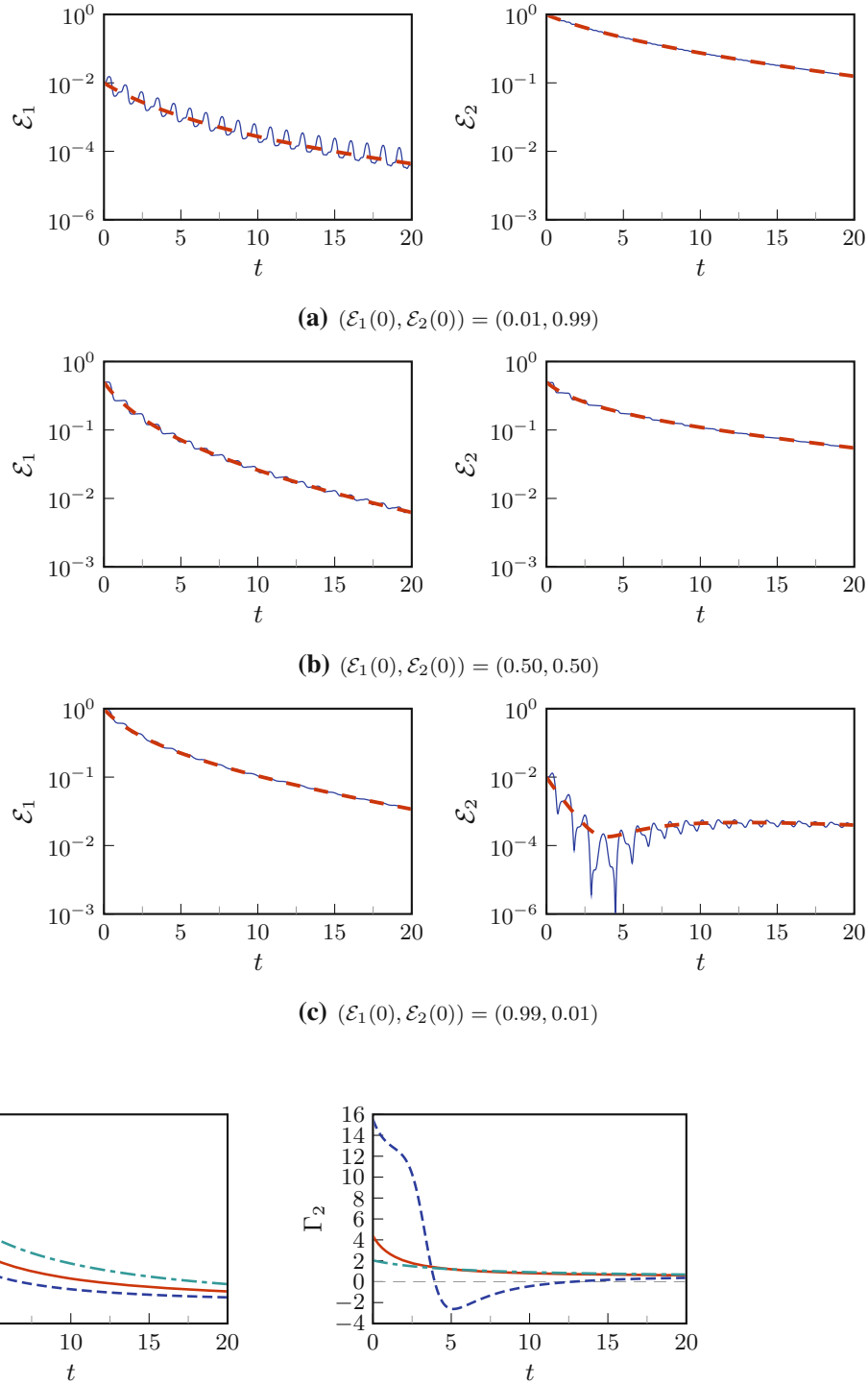

Fig. 5 Modal energies ($\gamma = 1/\sqrt{2}$, $\psi_{12}(0) = 0$, $(\mathcal{E}_1(0), \mathcal{E}_2(0)) = (0.50, 0.50)$); Original Equations: blue solid line, averaged equations: red solid spaced line (Color figure online)

Fig. 6 Instantaneous damping, varying energy ratio ($\gamma = 1/\sqrt{2}$, $\psi_{12}(0) = 0$); $(\mathcal{E}_1(0), \mathcal{E}_2(0)) = (0.99, 0.01)$: blue dashed line, $(\mathcal{E}_1(0), \mathcal{E}_2(0)) = (0.50, 0.50)$: red solid line, $(\mathcal{E}_1(0), \mathcal{E}_2(0)) = (0.01, 0.99)$: green solid dotted line (Color figure online)

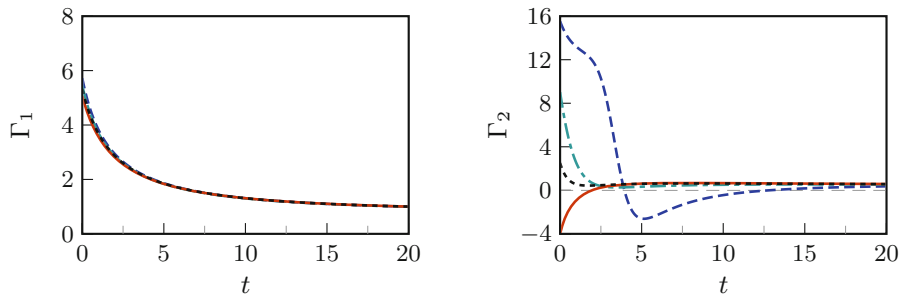

Fig. 7 Instantaneous damping, varying initial phase $\psi_{12}(0)$ ($\gamma = 1/\sqrt{2}$, $(\mathcal{E}_1(0), \mathcal{E}_2(0)) = (0.99, 0.01)$); $\psi_{12}(0) = 0$: blue dashed line, $\psi_{12}(0) = \pi/2$: green solid dotted line, $\psi_{12}(0) = \pi$: red solid line, $\psi_{12}(0) = 3\pi/2$: black dashed line (Color figure online)

decays and the corresponding decay rate is positive. However, near $t = 4$ the energy begins to increase, indicating that energy is transferred from Mode 1 to Mode 2 and the accompanying decay rate is negative. As time increases further, the energy finally begins to decay again. This response can be contrasted with that shown in Fig. 5a, where the energy is initially concentrated in Mode 2, so that $(\mathcal{E}_1(0), \mathcal{E}_2(0)) = (0.01, 0.99)$, but the effective damping in Mode 1 remains positive and no significant amount of energy is transferred between modes.

In contrast to the previous example with non-commensurate modes, the response of the modal amplitudes also depends on the resonant phase variable $\psi_{\alpha\beta}$, whose evolution is governed by Eq. (40). Moreover, the off-diagonal terms $\Lambda_{\alpha\beta}$ and $\Lambda_{\beta\alpha}$ can be of either sign, so that these terms allow for the exchange of energy between modes, depending on the resonant phase variable. As illustrated in Fig. 7, this can have a significant effect on the effective damping, in particular for Mode 2, although Mode 1 is relatively insensitive to the initial phase due to the relatively insignificant amount of energy in More 2. In each figure the effective damping is shown as the initial phase $\psi_{\alpha\beta}(0)$ varies. For example, with $\psi_{12}(0) = \pi$ the energy in Mode 2 initially grows due to mode coupling, so that Γ_2 is initially negative. Note that since these off-diagonal terms are dependent only on the energy in the lowest mode, these effects are most significant when this mode is active.

3 Conclusions

This analysis provides a description of energy transfer in the transient response of general resonant multi-degree-of-freedom system due to nonlinearities, and in particular the effect of mode coupling in the transient response of systems with light, generalized linear damping, linear detuning, and cubic nonlinearities. For the case of nonlinear systems, an approximate description of the instantaneous damping measure can be derived from the method of multiple scales; further, this approximate description directly shows how the instantaneous damping can be thought of as being energy-dependent. Moreover, the response of any mode of the system is shown to be dependent of the energy distribution throughout the system even when the modes are not commensurate. However, for the case of non-commensurate frequencies, this approximate damping term cannot become negative, implying that energy cannot be transferred from mode to mode; rather, the mode coupling only serves to increase the rate of energy dissipation in each mode. In contrast, when internal resonances are introduced to a system, asymmetric, potentially non-positive terms emerge in the nonlinear effective damping matrix that are directly responsible for modal energy transfer and non-reciprocal effects, that is, the nonlinearities allow for the energy of resonant modes to increase due to energy exchange. The asymmetric structure of the matrix allows for energy to easily transfer from low modes to high modes, but attenuates the transfer of energy from high modes to low modes, an effect commonly seen in experimentation and numerical studies.

Funding This research was supported by the Laboratory Directed Research and Development program at Sandia National Laboratories, a multimission laboratory managed and operated by National Technology and Engineering Solutions of Sandia, LLC., a wholly owned subsidiary of Honeywell International, Inc., for the U.S. Department of Energy's National Nuclear Security Administration under contract DE–NA–0003525.

Compliance with ethical standards

Conflict of interest The authors declare that they have no conflict of interest.

A Appendix

The coefficients $I^{\bullet,\bullet}_{ijkl}$ identified in Eq. (24) are defined as the Fourier components of terms in the slow-flow equations arising from the cubic nonlinearities. With $\psi_q \equiv \omega_q\,\eta_0 + \phi^{(0)}_q$, these reduce to

$$I^{s,\cos}_{ijkl} \equiv \frac{\omega_i}{\pi}\int_0^{2\pi/\omega_i} \left\{\cos\psi_i\ \sin\psi_j\ \sin\psi_k\ \sin\psi_l\right\} d\eta_0, \tag{42a}$$

$$I^{c,\cos}_{ijkl} \equiv \frac{\omega_i}{\pi}\int_0^{2\pi/\omega_i} \left\{\cos\psi_i\ \cos\psi_j\ \cos\psi_k\ \sin\psi_l\right\} d\eta_0, \tag{42b}$$

$$I^{v,\cos}_{ijkl} \equiv \frac{\omega_i}{\pi}\int_0^{2\pi/\omega_i} \left\{\cos\psi_i\ \sin\psi_j\ \sin\psi_k\ \cos\psi_l\right\} d\eta_0, \tag{42c}$$

$$I^{d,\cos}_{ijkl} \equiv \frac{\omega_i}{\pi}\int_0^{2\pi/\omega_i} \left\{\cos\psi_i\ \cos\psi_j\ \cos\psi_k\ \cos\psi_l\right\} d\eta_0, \tag{42d}$$

$$I^{s,\sin}_{ijkl} \equiv \frac{\omega_i}{\pi}\int_0^{2\pi/\omega_i} \left\{\sin\psi_i\ \sin\psi_j\ \sin\psi_k\ \sin\psi_l\right\} d\eta_0, \tag{42e}$$

$$I^{c,\sin}_{ijkl} \equiv \frac{\omega_i}{\pi}\int_0^{2\pi/\omega_i} \left\{\sin\psi_i\ \cos\psi_j\ \cos\psi_k\ \sin\psi_l\right\} d\eta_0, \tag{42f}$$

$$I^{v,\sin}_{ijkl} \equiv \frac{\omega_i}{\pi}\int_0^{2\pi/\omega_i} \left\{\sin\psi_i\ \sin\psi_j\ \sin\psi_k\ \cos\psi_l\right\} d\eta_0, \tag{42g}$$

$$I^{d,\sin}_{ijkl} \equiv \frac{\omega_i}{\pi}\int_0^{2\pi/\omega_i} \left\{\sin\psi_i\ \cos\psi_j\ \cos\psi_k\ \cos\psi_l\right\} d\eta_0, \tag{42h}$$

The evaluation of these integrals depends on the relationship between the frequencies $(\omega_i, \omega_j, \omega_k, \omega_l)$. Specifically, there exist terms that appear for any set of frequencies. For example,

$$I^{d,\cos}_{iiii} = \frac{3}{8}, \quad I^{d,\cos}_{iijj} = I^{d,\cos}_{ijij} = I^{d,\cos}_{ijji} = \frac{1}{4}, \tag{43}$$

while $I^{d,\cos}_{ijkl} = 0$ otherwise. Likewise one can show that $I^{d,\sin}_{ijkl} \equiv 0$. However, additional terms arise when there exists a $3:1$ resonance between two modal frequencies. For example, if α and β denote mode numbers such that $3\,\omega_\alpha = \omega_\beta$, then there are additional components of $I^{d,\cos}$ and $I^{d,\sin}$ such that

$$\begin{aligned} I^{d,\cos}_{\beta\alpha\alpha\alpha} &= I^{d,\cos}_{\alpha\beta\alpha\alpha} = I^{d,\cos}_{\alpha\alpha\beta\alpha} = I^{d,\cos}_{\alpha\alpha\alpha\beta} = \frac{1}{8}\cos\left(\psi^{(0)}_{\alpha\beta}\right), \\ -I^{d,\sin}_{\beta\alpha\alpha\alpha} &= I^{d,\cos}_{\alpha\beta\alpha\alpha} = I^{d,\cos}_{\alpha\alpha\beta\alpha} = I^{d,\cos}_{\alpha\alpha\alpha\beta} = \frac{1}{8}\sin\left(\psi^{(0)}_{\alpha\beta}\right), \end{aligned} \tag{44}$$

where $\psi^{(0)}_{\alpha\beta} \equiv 3\,\phi^{(0)}_\alpha - \phi^{(0)}_\beta$. These are in addition to the terms that exist for any set of frequencies. Similar conclusions hold for the remaining parameters.

References

1. Akulenko, L.D., Korovina, L.I., Kumakshev, S.A., Nesterov, S.V.: Self-sustained oscillations of Rayleigh and van der Pol oscillators with moderately large feedback factors. J. Appl. Math. **68**(2), 241–248 (2004)
2. Bilbao, A., Aviles, R., Agirrebeitia, J., Ajuria, G.: Proportional damping approximation for structures with added viscoelastic dampers. Finite Elem. Anal. Des. **42**, 492–502 (2006)
3. Chatterjee, S., Dey, S.: Nonlinear dynamics of two harmonic oscillators coupled by Rayleigh type self-exciting force. Nonlinear Dyn. **72**, 113–128 (2013)
4. Fuellekrug, U.: Computation of real normal modes from complex eigenvectors. Mech. Syst. Signal Process. **22**, 57–65 (2007)
5. Garvey, S., Penny, J., Friswell, M.: The relationship between the real and imaginary parts of complex modes. J. Sound Vib. **212**(1), 75–83 (1998)
6. Gottleib, O., Habib, G.: Non-linear model-based estimation of quadratic and cubic damping mechanisms governing the ddynamic of a chaotic spherical pendulum. J. Vib. Control **18**(4), 536–547 (2011)
7. Guckenheimer, J., Holmes, P.J.: Nonlinear Oscillations, Dynamical Systems, and Bifurcations of Vector Fields. Number 42 in Applied Mathematical Sciences. Springer, New York (1983)
8. Güttinger, J., Noury, A., Weber, P., Eriksson, A.M., Lagoin, C., Moser, J., Eichler, C., Wallraff, A., Isacsson, A., Bachtold, A.: Energy-dependent path of dissipation in nanomechanical resonators. Nat. Nanotechnol. **12**, 631–636 (2017)
9. Karabalin, R.B., Cross, M.C., Roukes, M.L.: Nonlinear dynamics and chaos in two coupled nanomechanical resonators. Phys. Rev. B **79**, 165309 (2009)
10. Kasai, T., Link, M.: Identification of non-proportional modal damping matrix and real normal modes. Mech. Syst. Signal Process. **16**(6), 921–934 (2002)
11. Lifshitz, R., Cross, M.C.: Response of parametrically driven nonlinear coupled oscillators with application to micromechanical and nanomechanical resonator arrays. Phys. Rev. B **67**, 134302 (2003)
12. Matheny, M.H., Villanueva, L.G., Karabalin, R.B., Sader, J.E., Roukes, M.L.: Nonlinear mode-coupling in nanomechanical systems. Nano Lett. **13**, 1622–1626 (2013)
13. Menottu, M., Morrison, B., Tan, K., Vernon, Z., Sipe, J.E., Liscidini, M.: Nonlinear coupling of linearly uncoupled resonators. Phys. Rev. Lett. **122**, 013904 (2019)

14. Moeck, J.P., Durox, D., Schuller, T., Candel, S.: Nonlinear thermoacoustic mode synchronization in annular combustors. Proc. Combust. Inst. **37**, 5343–5350 (2019)
15. Mook, D., Plaut, R., HaQuang, N.: The influence of an internal resonance on non-linear structural vibrations under subharmonic resonance conditions. J. Sound Vib. **102**(4), 473–492 (1985)
16. Nayfeh, A.H., Mook, D.T.: Nonlinear Oscillations. Wiley, New York (1995)
17. Pak, C.H.: On the coupling of non-linear normal modes. Int. J. Non-Linear Mech. **41**, 716–725 (2006)
18. Pak, C.H., Lee, Y.S.: Bifurcation of coupled-mode responses by modal coupling in cubic nonlinear systems. Q. Appl. Math. **74**(1), 1–26 (2016)
19. Rayleigh, J.W.S.B.: Theory of Sound. Dover Publications, New York (1877)
20. Remick, K., Joo, H.K., McFarland, D.M., Sapsis, T.P., Bergman, L., Quinn, D.D., Vakakis, A.: Sustained high-frequency energy harvesting through a strongly nonlinear electromechanical system under single and repeated impulsive excitations. J. Sound Vib. **333**, 3214–3235 (2014)
21. Udwadia, F.E.: A note on nonpropotional damping. J. Eng. Mech. **135**(11), 1248–1256 (2009)
22. Vakakis, A.F., Manevitch, L.I., Mikhlin, Y.V., Pilipchuk, V.N., Zevin, A.A.: Normal Modes and Localization in Nonlinear Systems. Wiley Series in Nonlinear Science. Wiley, New York (1996)